Polymer Testing 131 (2024) 108339

Contents lists available at ScienceDirect

Polymer Testing

journal homepage: www.elsevier.com/locate/polytest

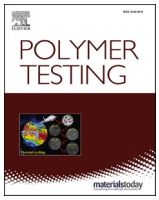

Kinetic mathematical model with induction and reversion for the vulcanization of natural rubber and ethylene propylene diene monomer blend

G. Pianese [a,*], G. Milani [a], F. Milani [b]

[a] Department of Architecture, Built Environment and Construction Engineering, Politecnico di Milano, Milano, Italy
[b] Chem. Co Consultant, Occhiobello, RO, Italy

ARTICLE INFO

Keywords:
Rheometer test
Induction
Reversion
Kinetic model
Numerical modeling
Rubber optimal vulcanization

ABSTRACT

The complexity inherent in modeling and optimizing rubber cure processes stems from the intricate interplay between "induction" and "reversion" phenomena. During the vulcanization process, rubber compounds undergo a gradual initial decrease in torque in an "induction" phase. Following this, the primary vulcanization reaction triggers a swift surge in cross-link density. Interestingly, the density may peak and subsequently decline, leading to compromised mechanical properties with prolonged curing times. This "reversion" phenomenon is extensively documented in sulfur-cured rubbers at elevated vulcanization temperatures, typically exceeding 140 °C. Moreover, the cure conditions can influence the final structure, mechanical performance, and thermal stability of the network.

This paper introduces a kinetic mathematical model that is able to predict the optimal time and temperature for a blend of natural rubber and ethylene propylene diene monomer. This model incorporates considerations for both the induction and reversion phases of the vulcanization process. These considerations prove particularly critical, especially in scenarios involving large rubber items or when the rheometer curves of the rubber exhibit a slow pace with significant reversion towards the end. Additionally, the study proposes a novel approach for determining the kinetic variables that concurrently consider all vulcanization temperatures using a standard genetic algorithm.

1. Introduction

Rubber, a versatile material, has extensive applications in household and industrial settings. Its history traces back to prehistoric times when humans harnessed latex from specific trees [1]. The industrial use of rubber commenced in the early 18th century. In contemporarily times, rubber is prevalent in various applications such as tires, vibration or seismic isolators, impermeable layers, and sports equipment. It exists in either natural (NR) or synthetic forms, with notable synthetic types including Hypalon, Ethylene Propylene Diene Monomer (EPDM), Nitrile-Butadiene Rubber (NBR), Viton, Neoprene, Silicone rubber (SiR), and Styrene-Butadiene Rubber (SBR).

Vulcanization, a crucial process, induces the formation of cross-links between elongated rubber molecules, resulting in a polymer network. These cross-links prevent the chains from sliding along each other, rendering the rubber elastic. Determining optimal curing times and temperatures is essential for the effective development of the polymer network, ensuring that the rubber exhibits excellent mechanical properties. The mechanical characteristics of rubber are significantly influenced by the curing temperature and time [2]. Over-curing, for instance, can lead to reversion in NR (a notable issue), causing the breakdown of transversal cross-links and a subsequent decline in key mechanical properties. Conversely, an under-cured sample will lack optimum mechanical characteristics, exhibiting inferior performance [3]. In general, the vulcanization process with sulfur unfolds in three distinct steps: "induction", "cross-linking", and "post-crosslinking". This conceptual framework stems from a macroscopic interpretation of events occurring in a sample during controlled temperature curing conditions in the rheometer chamber.

The rheometer curve (Fig. 1) represents the torque resistance of a sample undergoing a fixed-temperature cure over time. Initially, there is a slight decrease in torque, known as the "induction" phase (blue).

* Corresponding author.
E-mail address: gaetano.pianese@polimi.it (G. Pianese).

https://doi.org/10.1016/j.polymertesting.2024.108339
Received 16 November 2023; Received in revised form 20 December 2023; Accepted 11 January 2024
Available online 23 January 2024

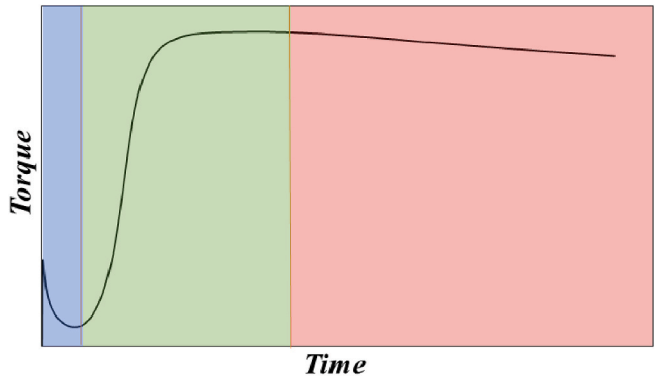

Fig. 1. Rheometer curve: induction (blue), vulcanization (green), and post-vulcanization (red). (For interpretation of the references to colour in this figure legend, the reader is referred to the Web version of this article.)

Following this, a rapid cross-link formation occurs, marked by a significant torque increase called "polymerization" (green). Eventually, there is a final degradation at sufficiently extended vulcanization times, resulting in a torque decrease, commonly termed "reversion" (red).

During the "induction" period, the cross-link density of rubber compounds experiences a gradual initial increase. Subsequently, the main vulcanization reaction ensues, characterized by a notably faster rise in cross-link density. In contrast, "reversion" entails a significant reduction in rubber vulcanized properties towards the end of the curing process. This phenomenon is influenced by various factors, with the rubber type and vulcanization temperature being among the most critical.

As comprehension of the nature of the reaction has advanced, the kinetic approach has emerged as a viable means of predicting vulcanization. This methodology involves establishing mathematical relationships between the degree of cure and time, capable of fitting experimental data when a chemical reaction scheme is postulated and translated into mathematical differential relations.

Ding and Leonov [4] were among the pioneers to introduce a sophisticated kinetic scheme for NR, aiming to elucidate the processes of induction, cross-linking, and reversion. Their approach primarily relies on the summation of exponential laws, where distinct kinetic constants, derived from the simplified kinetic scheme proposed by Coran [5], govern cross-linking and devulcanization.

Han et al. [6] provided a plausible description of reversion, utilizing a reduced number of kinetic parameters with physical significance. They posited that, during vulcanization, first-order reactions can form stable and unstable sulfur cross-links after an initial induction period with no cross-linking reaction. The latter are susceptible to subsequent degradation due to another first-order reaction. This model underwent partial modifications by Leroy et al. [7] and further adjustments by Milani et al. [8], resulting in a comprehensive mathematical model with seven kinetic constants. The model, with a foundation in kinetics, is designed to predict the vulcanization degree of natural rubber (NR) treated with sulfur, employing a highly refined methodology. It exclusively requires rheometer curves as input for fitting and yields kinetic constants representing the intricate individual reactions within the cross-linking process. To overcome the primary constraint of the Milani et al. [8] approach, characterized by inherent complexity that hinders the manipulation of closed-form functions for the cross-linking degree, Milani and Milani [9] undertook a simplification of the kinetic scheme. Despite this streamlining, their model effectively fits experimental data while facilitating the rigorous derivation of a closed-form solution for the curing degree. However, a notable drawback in this latter approach is the determination of unknown kinetic constant parameters, necessitating the utilization of non-linear least-squares fitting. This process heavily relies on the initial starting point, a critical consideration in the success of least-squares minimization, particularly in dealing with multivariable problems. In certain instances, the algorithm may encounter challenges in identifying the optimal solution or require computationally intensive time resources.

In this paper, a kinetic mathematical model to predict the optimal vulcanization is presented. Compared to the previous work [2], here, the new numerical model takes into account the "induction" and the "reversion". Furthermore, an optimization procedure for the evaluation of the kinetic constants is proposed, where all vulcanization temperatures are considered contemporarily. The variability of the kinetic constants with the temperature is classically assumed to be ruled by an Arrhenius law. The experimental rheometer data fitting is then performed with a Genetic Algorithm (GA). To evaluate the outcomes achieved with the proposed model, a set of experimental data sourced from previous research [2] has been considered. They consist of four rheometer curves obtained from a NR-EPDM blend recorded at various temperatures. These curves show reversion as the temperature is raised to 170 °C. The method showcased remarkable speed and dependability, providing results of utmost precision. This strategy is adaptable and suitable for various rubber compounds, contingent on the availability of pertinent but constrained experimental data to characterize cross-linking reactions across diverse temperatures.

Table 1
NR-EPDM composition.

Ingredient	Parts per hundred rubber (PHR)	%
NR	60.00	22.50
EPDM Vistalon 3666	70.00	28.60
ZnO	5.00	2.00
Carbon Black	60.00	24.50
Silica	15.00	6.10
Naphthenic oil	10.00	3.05
Accelerators	13.80	5.50
Sulfur	1.50	0.60
Others	15.12	7.15

Table 2
Vistalon 3666 properties.

Parameters	Typical Value
Propylene Content	32 wt%
ENB (5-ethyliden-2-norbornene) Content	4.5 wt%
Oil Content	42 wt%
ML (1+4) 100 °C	71 MU
ML (1+4) 121 °C	53 MU
Molecular weight distribution (MWD)	Medium/Large
Green Strenght (GS)	5.1 kg/cm^2

2. Rubber compound used to test the numerical model

Table 1 presents the NR-EPDM composition under consideration for this study. The blend includes the use of commercial EPDM Vistalon 3666, known for its extended oil, medium/large molecular weight distribution, 4.5 % by weight ENB (5-ethyliden-2-norbornene) content, and a 32 % weight propylene content (refer to Table 2 for additional details). This NR-EPDM blend results from an extensive numerical and experimental investigation [2,10], wherein various rubber compounds were characterized. The ultimate goal was to formulate a rubber compound suitable for high-damping elastomeric isolators. In contrast to the conventional NR or polychloroprene rubber employed in the manufacture of elastomeric seismic isolators, as recommended by the European code for anti-seismic devices [11], the use of synthetic rubbers have been contemplated. NR displays promise in terms of mechanical properties, but it is hampered by inadequate damping capabilities and rapid aging [12]. Combining NR with synthetic rubbers, such as EPDM, led to final rubber compounds exhibiting good overall mechanical properties,

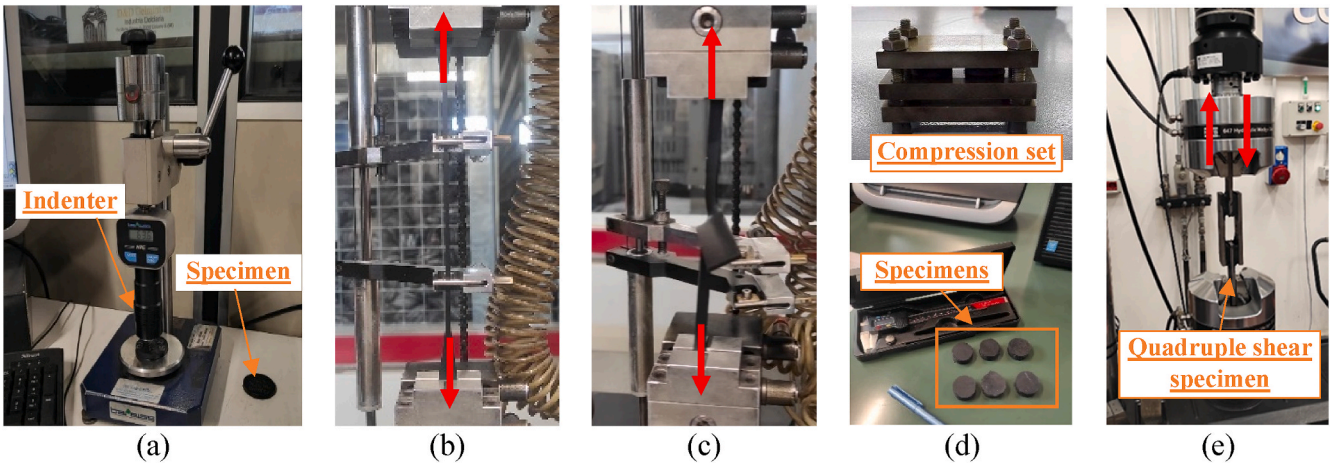

Fig. 2. Rubber compound characterization: hardness measurement (a), uniaxial tensile test (b), tear resistance test (c), compression set (d), and quadruple shear test (e).

effective damping capacity, and enhanced durability [13–16]. Beyond that, exploring alternative rubber blends opens avenues for incorporating recycled rubber compositions [3,17–19]. Notably, synthetic rubbers like EPDM show promise for such applications, as the final recycled rubber compound mirrors the characteristics of virgin rubber [20].

In detail, in the previous work [2,10], seven rubber compositions were proposed and characterized according to the European code for anti-seismic devices [11]. This involved conducting Shore A hardness, uniaxial tensile, tear resistance, compression set, accelerated aging, and quadruple shear tests.

The Shore A hardness test (Fig. 2a) is a widely used method for gauging the hardness of rubber. It assesses the resistance of the material to penetration by an indenter, with hardness expressed in dimensionless Shore A units (ShA) ranging from 0 to 100 [21]. A Shore A value of 0 signifies a fully soft, unvulcanized material, while a value of 100 indicates a completely hard material. The results of the test are inversely related to penetration and rely on the modulus of elasticity and viscoelastic properties of the material.

The uniaxial tensile test is employed to assess the mechanical properties of rubber and elastomer materials. Using a dumbbell specimen (Fig. 2b), the material is clamped between grips on a testing machine, applying a steadily increasing force until the sample breaks [22]. The machine records applied force, elongation, or deformation throughout the test. Key mechanical properties, such as tensile strength at break, elongation at break, and modulus of elasticity, can be calculated from these measurements. Tensile strength at break (TS_{break}) denotes the maximum stress the material can endure before breaking, elongation at break (E_{break}) signifies the percentage of deformation before breakage, and the modulus of elasticity (E) gauges material stiffness and it is calculated as the slope in the linear elastic region of the stress-strain curve.

The tear resistance test evaluates the ability of rubber materials to withstand tearing. In the trousers tear test, a rectangular sample is cut, and a small slit is made at the center of one longer edge (depth of 40 ± 5 mm) [23]. The sample is inserted into a tensile-testing machine (Fig. 2c), initiating the test while monitoring changes in length and force. Tear strength (TS) is determined as the ratio of the maximum force recorded during the test to the thickness of the specimen.

The compression set assesses the ability of the rubber material to regain its original shape after compression. In this test, a rubber sample is compressed between two parallel plates to 9.75 mm and held at 70 °C for 24 h (Fig. 2d) [24]. After compression, the sample is released and allowed to recover for 30 min, and its thickness is measured. The compression set (CS) is then calculated as the percentage difference between the initial thickness (T_i) and the thickness after recovery (T_f), relative to the thickness during compression (T_d), using the formula $\frac{T_i - T_f}{T_i - T_d} * 100$.

Accelerated aging tests assess the long-term durability and aging behavior of elastomeric materials by exposing them to 70 °C for 168 h. After this exposure, following the UNI EN 15129 [11] code, uniaxial tensile and hardness tests are conducted. The specimens from accelerated aging are tested at room temperature after 24 h of storage. As per the code, recommended maximum variations in hardness (ΔH), tensile strength (ΔTS_{break}), and elongation at break (ΔE_{break}) should not exceed −5 or +8 ShA, ±15 %, and ±25 %, respectively.

Ultimately, the cyclic shear test allows for the assessment of dynamic properties in rubber compounds. Utilizing the quadruple shear specimen (Fig. 2e), the test involves subjecting it to a 0.5 Hz cyclic shear amplitude for four complete sinusoidal cycles. From this test, valuable parameters such as the damping ratio and shear modulus can be derived. These parameters hold particular significance, especially during the design phase of the ultimate elastomeric rubber devices [25–27].

The detailed findings of this study can be found in Refs. [2,10], where readers are directed to a comprehensive understanding of the equipment and methods. Table 3 provides a summarized overview of the key mechanical and physical properties of the NR-EDPM blend, which has met all the minimum requirements of the code and has been considered for the study.

To assess the impact of various temperatures on the vulcanization, rheometric tests were conducted on the NR-EPDM blend at four distinct temperatures: 140 °C, 150 °C, 160 °C, and 170 °C. An oscillating disc rheometer (ODR) at 3° of arc has been used. The rheometer test measures the viscoelastic properties of rubber compounds during the

Table 3
Mechanical and physical properties of the rubber compound.

Density	Hardness	TS_{break}	E_{break}	E	TS	CS	G	Accelerated air oven aging			ξ
								ΔH	ΔTS_{break}	ΔE_{break}	
[g/cm3]	[ShA]	[MPa]	[%]	[MPa]	[kN/m]	[%]	[MPa]	[ShA]	[%]	[%]	[%]
1.129	60	16.06	620	1.63	22.8	35	0.77	+1	−4.51	−9	8.4

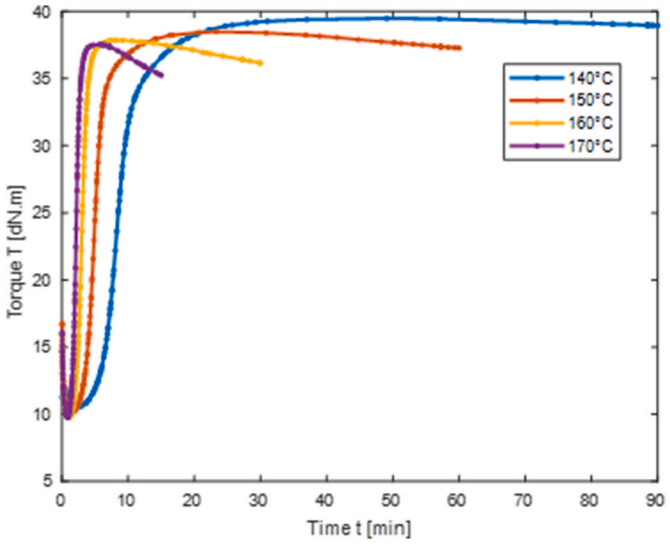

Fig. 3. NR-EPDM rheometer curves at different temperatures.

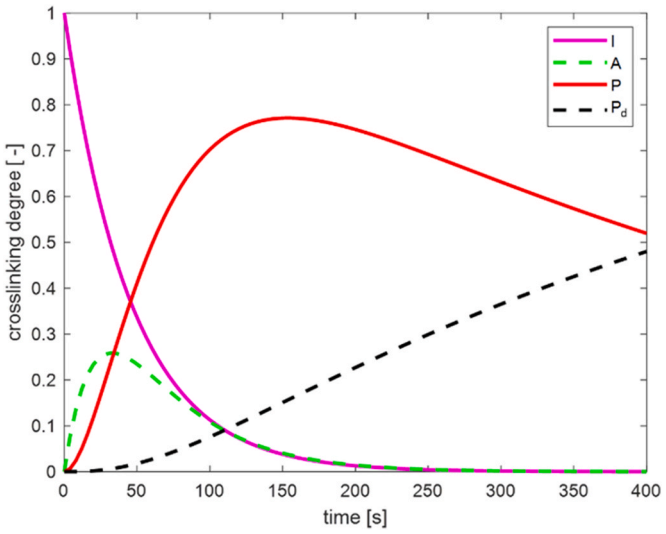

Fig. 4. Model results when Ka = 0.0218 s−1, Kp = 0.0412 s−1 and Kr = 0.002 s−1.

vulcanization process. The minimum torque recorded on the curve, denoted as *ML*, signifies the stiffness of uncured rubber at a specific temperature. As the curing process initiates, the torque ascends. T_{S2}, representing the time taken for the torque to increase by two units above the *ML* value, typically delineates the scorch time—the point at which vulcanization commences. This parameter, crucial for defining the induction time of rubber compounds, is often overlooked in determining the optimal vulcanization time and temperature. However, in cases involving prolonged vulcanization induction times and substantial dimensions of rubber items, T_{S2} becomes indispensable and necessitates consideration. As the curing advances, the torque continues to rise. The peak torque recorded on the curve is termed *MH*. T_{90} denotes the time from the commencement of the test to the point where 90 % of the MH value is attained. The same description applies to T_{10} and T_{50}. M_{final} is the value of the torque at the end of the test.

As depicted in Fig. 3 and detailed in Table 4, the elevation in the vulcanization temperature quickens the curing process and intensifies reversion. This is an undesirable trait in rubber, potentially leading to a reduction in mechanical properties and an overall decline in material performance [28]. It has been calculated as the ratio between the difference of M_H and M_{final}, and the M_H ($\frac{M_H - M_{final}}{M_H}$). While NR typically exhibits reversion in the range of 30–35 %, the NR-EPDM blend here displays a lower reversion, specifically 5.84 % at the maximum temperature. The vulcanization process at 140 °C appears to be the most favorable, yielding the highest *MH*. Conversely, vulcanization at 170 °C resulted in the lowest *MH*.

3. Rubber vulcanization

3.1. Kinetic model

To predict the curing behavior of rubber, let us consider the following complex scheme with three reactions occurring in series:

$$I \xrightarrow{K_a} A \xrightarrow{K_p} P \xrightarrow{K_r} P_d \tag{1}$$

where I is the rubber inducted, A is the rubber activated, P is the cured polymer, P_d is the devulcanized part of rubber, K_a is the activated rubber kinetic constant, K_p is the secondary polymerization kinetic constant and K_r the devulcanization constant, measuring reversion. The three reactions occur with a kinetic velocity depending on the temperature reaction associated with the two kinetic constants. Differential equations associated with chemical reactions (*I-A-P-*P_d) are the following:

$$\begin{cases} \dfrac{dI}{dt} = -K_a I \\ \dfrac{dA}{dt} = K_a I - K_p A \\ \dfrac{dP}{dt} = K_p A - K_r P \\ \dfrac{dP_d}{dt} = K_r P \end{cases} \tag{2}$$

When K_a, K_p and K_r do not depend on T, or T is constant (rheometer test), a closed form solution exists.

Indeed, Eq. (2) is a first order linear homogeneous system of partial differential equations that can be re-written in matrix form as follows:

$$\frac{d}{dt}\begin{bmatrix} I \\ A \\ P \\ P_d \end{bmatrix} = \begin{bmatrix} -K_a & 0 & 0 & 0 \\ K_a & -K_p & 0 & 0 \\ 0 & K_p & -K_r & 0 \\ 0 & 0 & K_r & 0 \end{bmatrix} \begin{bmatrix} I \\ A \\ P \\ P_d \end{bmatrix} = \boldsymbol{K} \begin{bmatrix} I \\ A \\ P \\ P_d \end{bmatrix} \tag{3}$$

Problem (3) can be re-written in compact matrix notation as follows:

$$\frac{d\boldsymbol{X}}{dt} = \boldsymbol{K}\boldsymbol{X} \tag{4}$$

Where $\boldsymbol{X} = [I \quad A \quad P \quad P_d]^T$.

Table 4
Rheometer experimental results.

Test temp	Test time	ML	TS2	T10	T50	T90	MH	Mfinal	Reversion
[°C]	[min.ss]	[dNm]	[min.ss]	[min.ss]	[min.ss]	[min.ss]	[dNm]	[dNm]	[%]
140	90.00	11.93	5.29	5.59	8.31	15.01	44.61	44.01	1.34
150	60.00	11.55	3.14	3.29	4.59	7.50	43.49	42.12	3.17
160	30.00	11.03	1.58	2.07	3.01	3.59	42.24	40.85	3.29
170	12.00	10.80	1.19	1.25	2.01	2.40	42.22	39.75	5.84

Let's now change the coordinates by means of a linear transformation matrix so that:

$$\boldsymbol{X} = \boldsymbol{V}\boldsymbol{Z} \tag{5}$$

and so that the dynamics are diagonal:

$$\frac{d\boldsymbol{Z}}{dt} = \boldsymbol{D}\boldsymbol{Z} \tag{6}$$

where $\boldsymbol{D}$ is a diagonal matrix.

In fact, by substituting (5) into (4), we obtain:

$$\boldsymbol{V}\frac{d\boldsymbol{Z}}{dt} = \boldsymbol{K}\boldsymbol{V}\boldsymbol{Z} \tag{7}$$

$$\begin{cases} I = e^{-K_a t} \\ A = \dfrac{K_a}{K_a - K_p}\left(e^{-K_p t} - e^{-K_a t}\right) \\ P = K_a K_p \left[\dfrac{e^{-K_a t}}{(K_a - K_p)(K_a - K_r)} - \dfrac{e^{-K_p t}}{(K_a - K_p)(K_p - K_r)} + \dfrac{e^{-K_r t}}{(K_a - K_r)(K_p - K_r)}\right] \\ P_d = K_a K_r \dfrac{e^{-K_p t}}{(K_a - K_p)(K_p - K_r)} - K_p K_r \dfrac{e^{-K_a t}}{(K_a - K_p)(K_a - K_r)} - K_a K_p \dfrac{e^{-K_r t}}{(K_a - K_r)(K_p - K_r)} + 1 \end{cases} \tag{14}$$

$$\frac{d\boldsymbol{Z}}{dt} = \boldsymbol{V}^{-1}\boldsymbol{K}\boldsymbol{V}\boldsymbol{Z} \tag{8}$$

$$\boldsymbol{V}^{-1}\boldsymbol{K}\boldsymbol{V} = \boldsymbol{D} \tag{9}$$

It is worth noting that Eq. (9) is a typical diagonalization problem and matrices $\boldsymbol{V}$ and $\boldsymbol{D}$ appear as follows:

$$\boldsymbol{V} = \begin{bmatrix} \boldsymbol{v}_1 & \boldsymbol{v}_2 & \boldsymbol{v}_3 & \boldsymbol{v}_4 \end{bmatrix}$$
$$\mathbf{D} = \begin{bmatrix} \lambda_1 & 0 & 0 & 0 \\ 0 & \lambda_2 & 0 & 0 \\ 0 & 0 & \lambda_3 & 0 \\ 0 & 0 & 0 & \lambda_4 \end{bmatrix} \tag{10}$$

where $\boldsymbol{v}_i$ and λ_i are respectively the i-th eigen-vector and eigen-value of matrix $\boldsymbol{K}$.

The solution of Eq. (3) is therefore the following:

$$\begin{bmatrix} I \\ A \\ P \\ P_d \end{bmatrix} = C_1\,\boldsymbol{v}_1 e^{\lambda_1 t} + C_2\,\boldsymbol{v}_2 e^{\lambda_2 t} + C_3\,\boldsymbol{v}_3 e^{\lambda_3 t} + C_4\,\boldsymbol{v}_4 e^{\lambda_4 t} \tag{11}$$

where C_i are integration constants.

The following initial conditions allow to find C_i constants:

$$\begin{bmatrix} I \\ A \\ P \\ P_d \end{bmatrix}_{t=0} = \begin{bmatrix} 1 \\ 0 \\ 0 \\ 0 \end{bmatrix} \tag{12}$$

By solving the previous simple system of four linear equations, C_i constants can be determined as follows:

$$\begin{cases} C_1 = 1 \\ C_2 = -\dfrac{K_p K_r}{(K_a - K_p)(K_a - K_r)} \\ C_3 = \dfrac{K_a K_r}{(K_a - K_p)(K_p - K_r)} \\ C_4 = -\dfrac{K_a K_p}{(K_a - K_r)(K_p - K_r)} \end{cases} \tag{13}$$

Combining Eq. (13) with Eq. (11), then Eq. (11) can be re-written as follows:

P in Eq. (14) represents the vulcanization degree of the model. In presence of induction, before the induction time t_{in} the curing does not start, so:

$$P = 0 \qquad t < t_{in}$$
$$P = K_a K_p \left[\frac{e^{-K_a(t-t_{in})}}{(K_a-K_p)(K_a-K_r)} - \frac{e^{-K_p(t-t_{in})}}{(K_a-K_p)(K_p-K_r)} + \frac{e^{-K_r(t-t_{in})}}{(K_a-K_r)(K_p-K_r)}\right] \qquad t \geq t_{in} \tag{15}$$

For illustrative purposes, let us assume that the kinetic constants. K_a, K_p and K_r are respectively equal to 0.0218 s^{-1}, 0.0412 s^{-1} and 0.002 s^{-1}. The results obtained for I, A, P and P_d are shown in Fig. 4.

3.2. Experimental

Various measurements have been performed on a discrete experimental dataset of times t_i at each temperature (in this case four, equal to 140 °C, 150 °C, 160 °C and 170 °C). The raw data on torque $T(t_i)$ so obtained are then used to evaluate the evolution of the curing degree $\alpha_{exp}(t_i)$ according to the procedure proposed by Sun and Isayev [29], i.e. using the following formula:

$$\alpha_{exp}(t_i) = \frac{T(t_i) - T_{minT}}{T_{maxT_0} - T_{minT_0}} \tag{16}$$

In Eq. (16), apart from the symbols already defined, T_{minT} represents the minimum value of torque during a curing test in the rheometer at a temperature T, and T_{maxT_0} (T_{minT_0}) is the maximum (minimum) torque at the lowest vulcanization temperature T_0 (in this case 140 °C), low enough to consider the reversion phenomenon negligible. The resulting curing degree always turns out to be between 0 and 1, and it is a non-dimensional variable.

Raw torque data at the four vulcanization temperatures tested and the corresponding normalized ones (according to Eq. (16)) are depicted in Figs. 3 and 5, respectively.

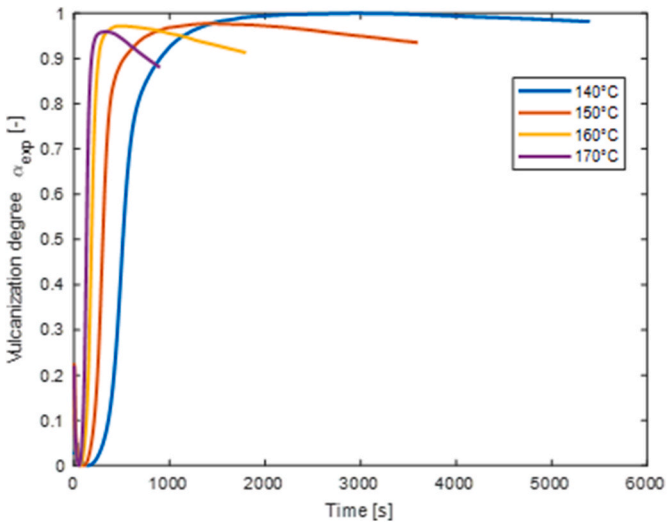

Fig. 5. Experimental rheometer curves after torque normalization

The variables to determine in the kinetic model are four, namely the induction time t_{in} and the three kinetic constants K_a, K_p and K_r. In Ref. [7] (and then, e.g., in Ref. [30]) it is assumed that the induction time is ruled by a reverse Arrhenius relationship in the following form:

$$t_{in}(T) = t_0 e^{\frac{E_{in}}{RT}} \tag{17}$$

Where t_0 is the induction at infinite temperature, E_{in} is the activation energy and R is the universal gas constant. It is also usually assumed that the kinetic constants follow a standard Arrhenius law, so that there is a linear relationship between the inverse of the absolute temperature and the logarithm of the kinetic constant in the so-called Arrhenius plane. Consequently, the dependence of K_a, K_p and K_r upon the vulcanization temperature is the following:

$$\begin{cases} K_a(T) = K_{a0} e^{-\frac{E_a}{RT}} \\ K_p(T) = K_{p0} e^{-\frac{E_p}{RT}} \\ K_r(T) = K_{r0} e^{-\frac{E_r}{RT}} \end{cases} \tag{18}$$

where, apart from the symbols already introduced, the others in Eq. (18) have the following meaning:

- E_a, E_p and E_r are the activation energies of K_a, K_p and K_r, respectively;
- K_{a0}, K_{p0}, K_{r0} are the values at an absolute temperature T equal to infinite of the K_a, K_p and K_r constants, respectively;

Substituting Eqs. (17) and (18) into Eq. (15), we obtain that the cross-linking degree is the following:

$$P(t) = \begin{cases} 0 & t < t_{in} \\ K_{a0} e^{\frac{E_a}{RT}} K_p \left[\begin{array}{l} \dfrac{e^{-K_a\left(t - t_0 e^{\frac{E_{in}}{RT}}\right)}}{\left(K_{a0} e^{-\frac{E_a}{RT}} - K_{p0} e^{-\frac{E_p}{RT}}\right)\left(K_{a0} e^{-\frac{E_a}{RT}} - K_{r0} e^{-\frac{E_r}{RT}}\right)} - \\ + \dfrac{e^{-K_{p0} e^{-\frac{E_p}{RT}}\left(t - t_0 e^{\frac{E_{in}}{RT}}\right)}}{\left(K_{a0} e^{-\frac{E_a}{RT}} - K_{p0} e^{-\frac{E_p}{RT}}\right)\left(K_{p0} e^{-\frac{E_p}{RT}} - K_{r0} e^{-\frac{E_r}{RT}}\right)} + \\ + \dfrac{e^{-K_r\left(t - t_0 e^{\frac{E_{in}}{RT}}\right)}}{\left(K_{a0} e^{-\frac{E_a}{RT}} - K_{r0} e^{-\frac{E_r}{RT}}\right)\left(K_{p0} e^{-\frac{E_p}{RT}} - K_{r0} e^{-\frac{E_r}{RT}}\right)} \end{array} \right] & t \geq t_{in} \end{cases} \tag{19}$$

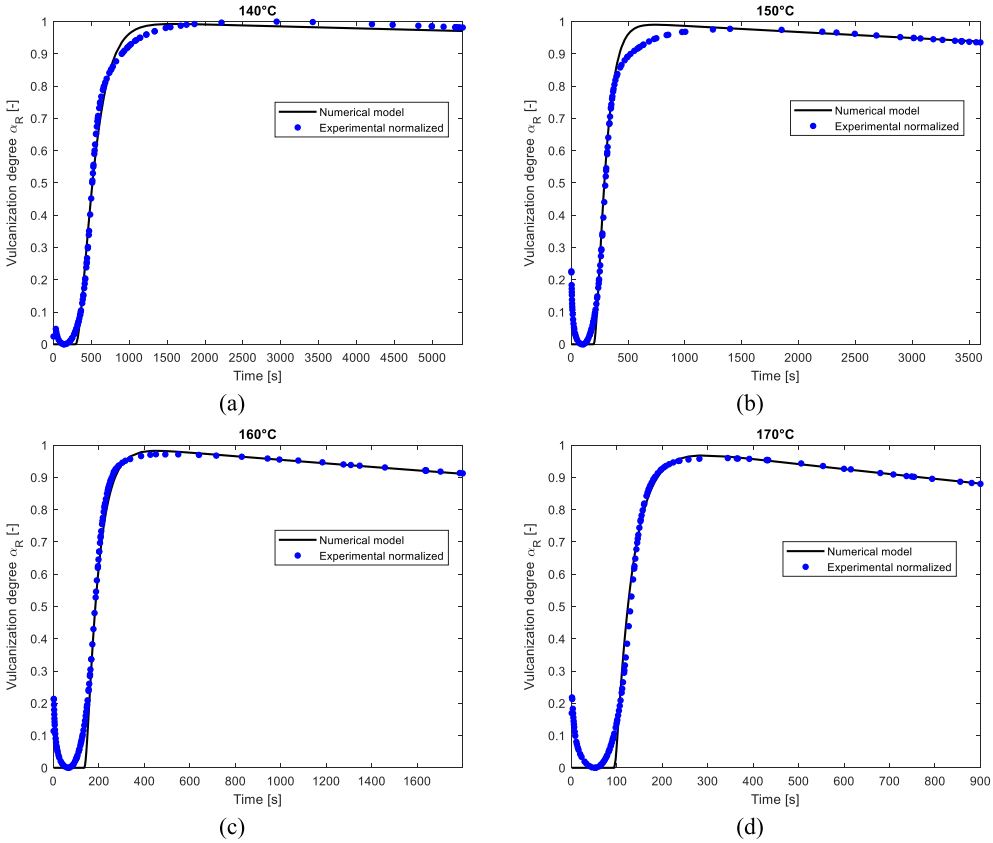

Fig. 6. Comparison between normalized experimental data and GA optimized numerical results at 140 °C(a), 150 °C (b), 160 (c), and 170 °C (d).

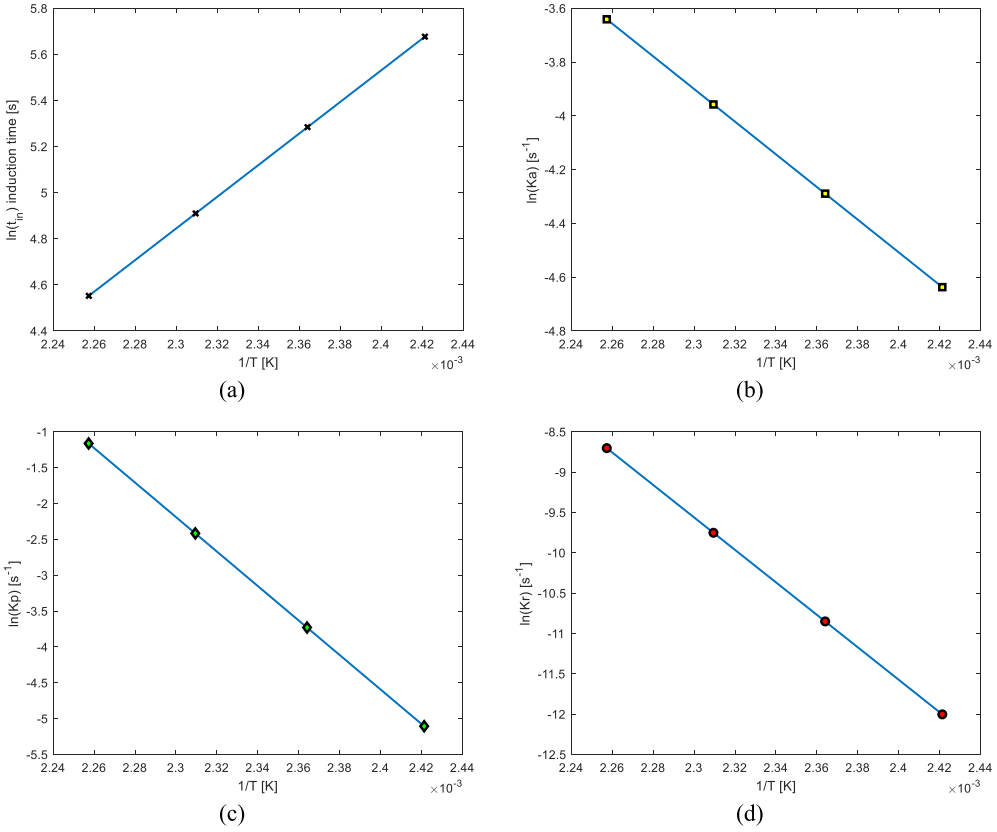

Fig. 7. Induction time t_{in} (a), kinetic constant K_a (b), kinetic constant K_p (c) and kinetic constant K_r (d), found through GA least squares optimization at four vulcanization temperatures.

Looking at Eq. (19), it turns out that the cross-linking degree at any temperature is univocally determined in the model when 8 parameters are known, namely t_0, E_{in}, E_a, E_p, E_r, K_{a0}, K_{p0} and K_{r0}. Typically, such parameters can be estimated numerically, considering them as optimization variables in a least squares minimization problem, where the cumulated square difference between numerical prediction and normalized experimental data is minimized upon the experimentally sampled points. In such technique, which should be considered a novelty in the state of the art, all vulcanization temperatures are considered here contemporarily, so the unconstrained objective function to minimize is the following:

$$O_{bj} = \sum_{k=1}^{4} \sum_{i=1}^{n_s} \left[P(t_i, T_k) - \alpha_{exp}(t_i, T_k) \right] \quad t_i \geq t_{in} \tag{20}$$

In the previous equation, the symbols have the following meaning:

- summation with index k refers to the temperatures tested;
- summation with index i refers to the points sampled at each temperature;
- n_s is the total number of sampled points at each temperature;
- $\alpha_{exp}(t_i, T_k)$ is the experimental value of the normalized torque at temperature T_k and at time t_i.

It is also worth noting that the least-squares minimization is carried out only for times after the induction t_{in}, because before, no sulfur cross-links are formed.

Nowadays, there are many numerical techniques to minimize Eq. (20), but in the presence of experimental data, for which a large discrete database is at disposal, meta-heuristic techniques probably appear to be the most efficient and straightforward. Classic gradient algorithms are not recommended because the problem is characterized by a multivariable objective function exhibiting many local minimum points where the kernel can easily remain trapped. For this reason, a robust GA is used [31]. The numerical normalized rheometer curves (continuous black curves) obtained are shown in Fig. 6 for the different temperatures investigated and compared with the normalized experimental data (blue dots). As can be noticed, the fitting capabilities of the model are rather good, and the reversion phenomenon is described accurately. Fig. 7 shows in the Arrhenius plane t_{in} (a), K_a (b), K_p (c) and K_r (d), calculated using Eqs. (17) and (18) using the optimal point variables (best individuals at the last iteration).

4. Conclusions

The paper introduced a kinetic model that allows for the prediction of vulcanization of sulfur-cured NR-EPDM blend, considering induction and reversion. In the initial phase of the investigation, the rubber compound underwent experimental characterization through various rheometer tests conducted at four different temperatures. The objective was to evaluate the influence of the temperature on the final vulcanization of the rubber. As expected, no reversion phenomena were observed at low temperatures (140-150 °C). Conversely, at higher temperatures (160-170 °C), the reversion phenomenon increased, resulting in a torque force decrease of approximately 5 %.

Based on the experimental data, the kinetic variables have been evaluated using as objective function the rheometer curves at all temperatures contemporarily. A novel approach was employed, utilizing a Genetic Algorithm least squares optimization. This optimization encompassed the kinetic constants and the induction time contemporarily for all the different vulcanization temperatures. After acquiring the kinetic variables, it became feasible to chart the developments of the

cross-linking degree at various temperatures. A comparison was made with experimental rheometer tests, revealing the precision of the model in making accurate predictions for both induction and reversion phenomena. This methodology proves particularly valuable in scenarios involving the production of sizable items or when working with rubber compounds that display significant induction and reversion characteristics.

CRediT authorship contribution statement

G. Pianese: Investigation, Methodology, Validation, Writing – original draft, Writing – review & editing, Conceptualization. **G. Milani:** Conceptualization, Investigation, Methodology, Supervision, Writing – review & editing, Validation. **F. Milani:** Conceptualization, Investigation, Methodology, Supervision, Validation.

Declaration of competing interest

The authors declare that they have no known competing financial interests or personal relationships that could have appeared to influence the work reported in this paper.

Data availability

Data will be made available on request.

References

[1] J.E. Mark, B. Erman, C.M. Roland, The Science and Technology of Rubber, fourth ed., 2013.

[2] G. Pianese, G. Milani, F. Milani, Prediction of the optimal vulcanization of a fiber-reinforced elastomeric isolator made of natural rubber-ethylene propylene diene monomer blend, Polym. Eng. Sci. 63 (2023) 2421–2443, https://doi.org/10.1002/pen.26386.

[3] A.B. Habieb, A. Formisano, G. Milani, G. Pianese, Seismic performance of Unbonded Fiber-Reinforced Elastomeric Isolators (UFREI) made by recycled rubber. Influence of suboptimal crosslinking, Eng. Struct. 256 (2022) 114038, https://doi.org/10.1016/j.engstruct.2022.114038.

[4] R. Ding, A.I. Leonov, A kinetic model for sulfur accelerated vulcanization of a natural rubber compound, J. Appl. Polym. Sci. 61 (1996), https://doi.org/10.1002/(sici)1097-4628 (19960718)61:3<455::aid-app8>3.3.co;2-h.

[5] A.Y. Coran, Vulcanization. Part V. The formation of crosslinks in the system: natural rubber-sulfur-MBT-zinc ion, Rubber Chem. Technol. 37 (1964), https://doi.org/10.5254/1.3540360.

[6] I.S. Han, C.B. Chung, S.J. Kang, S.J. Kim, H.C. Jung, A kinetic model of reversion type cure for rubber compounds, Polymer (Korea) 22 (1998).

[7] E. Leroy, A. Souid, R. Deterre, A continuous kinetic model of rubber vulcanization predicting induction and reversion, Polym. Test. 32 (2013) 575–582, https://doi.org/10.1016/j.polymertesting.2013.01.003.

[8] G. Milani, E. Leroy, F. Milani, R. Deterre, Mechanistic modeling of reversion phenomenon in sulphur cured natural rubber vulcanization kinetics, Polym. Test. 32 (2013), https://doi.org/10.1016/j.polymertesting.2013.06.002.

[9] G. Milani, F. Milani, Optimal vulcanization of tires: experimentation on idealized NR-PB natural and poly-butadiene rubber blends, phenomenological smoothed numerical kinetic model and FE implementation, Polym. Test. 72 (2018), https://doi.org/10.1016/j.polymertesting.2018.09.030.

[10] G. Pianese, N. Van Engelen, H. Toopchi-Nezhad, G. Milani, High-damping fiber-reinforced elastomeric seismic isolator in different boundary conditions: an experimental insight, Eng. Struct. 300 (2024) 117199, https://doi.org/10.1016/j.engstruct.2023.117199.

[11] European Committee for Standardization: EN 15129, Anti-seismic Devices, 2018.

[12] G. Wypych, Handbook of Polymers, third ed., 2022.

[13] K.S. Sisanth, M.G. Thomas, J. Abraham, S. Thomas, General introduction to rubber compounding, in: Progress in Rubber Nanocomposites, 2017.

[14] O. Ranaei, A.A. Aghakouchak, Experimental and numerical study on developed elastomeric layers based on natural and butyl matrix rubbers for viscoelastic dampers, Mech. Time-Dependent Mater. 26 (2022), https://doi.org/10.1007/s11043-021-09484-2.

[15] J.C. Li, H.S. Zhang, X.Y. Zhao, J.G. Jiang, Y.X. Wu, Y.L. Lu, L.Q. Zhang, T. Nishi, Development of high damping natural rubber/butyl rubber composites compatibilized by isobutylene-isoprene block copolymer for isolation bearing, Express Polym. Lett. 13 (2019), https://doi.org/10.3144/expresspolymlett.2019.58.

[16] R. Qin, R. Huang, X. Lu, Use of gradient laminating to prepare NR/ENR composites with excellent damping performance, Mater. Des. 149 (2018), https://doi.org/10.1016/j.matdes.2018.03.063.

[17] D. Losanno, F. Palumbo, A. Calabrese, T. Barrasso, N. Vaiana, Preliminary investigation of aging effects on recycled rubber fiber reinforced bearings (RR-FRBs), J. Earthq. Eng. 26 (2022), https://doi.org/10.1080/13632469.2021.1871683.

[18] A. Calabrese, M. Spizzuoco, G. Serino, G. Della Corte, G. Maddaloni, Shaking table investigation of a novel, low-cost, base isolation technology using recycled rubber, Struct. Control Health Monit. 22 (2015), https://doi.org/10.1002/stc.1663.

[19] M. Spizzuoco, A. Calabrese, G. Serino, Innovative low-cost recycled rubber-fiber reinforced isolator: experimental tests and Finite Element Analyses, Eng. Struct. 76 (2014) 99–111, https://doi.org/10.1016/j.engstruct.2014.07.001.

[20] A.B. Habieb, G. Milani, R. Cerchiaro, V. Quaglini, F. Milani, Numerical study on rubber compounds made of reactivated ethylene propylene diene monomer for fiber reinforced elastomeric isolators, Polym. Eng. Sci. 61 (2021) 258–277, https://doi.org/10.1002/pen.25573.

[21] International Organization for Standardization, ISO 48-4, Rubber, Vulcanized or Thermoplastic - Determination of Hardness - Part 4: Indentation Hardness by Durometer Method (Shore Hardness), 2018.

[22] International Organization for Standardization, ISO 37, Rubber, Vulcanized or Thermoplastic - Determination of Tensile Stress-Strain Properties, 2017.

[23] International Organization for Standardization, ISO 34-1, Rubber, Vulcanized or Thermoplastic - Determination of Tear Strength - Part 1: Trouser, Angle and Crescent Test Pieces, 2015.

[24] International Organization for Standardization: ISO 815-1, Rubber, Vulcanized or Thermoplastic - Determination of Compression Set - Part 1: at Ambient or Elevated Temperatures, 2019.

[25] J.M. Kelly, Aseismic base isolation: review and bibliography, Soil Dynam. Earthq. Eng. 5 (1986), https://doi.org/10.1016/0267-7261(86)90006-0.

[26] J.M. Kelly, The role of damping in seismic isolation, Earthq. Eng. Struct. Dynam. 28 (1999) 3–20, https://doi.org/10.1002/(SICI)1096-9845 (199901)28:1<3::AID-EQE801>3.0.CO;2-D.

[27] K.N. Kalfas, N. Ghorbani Amirabad, D. Forcellini, The role of shear modulus on the mechanical behavior of elastomeric bearings when subjected to combined axial and shear loads, Eng. Struct. 248 (2021) 113248, https://doi.org/10.1016/j.engstruct.2021.113248.

[28] G. Milani, F. Milani, Kinetic finite element model to optimize sulfur vulcanization: application to extruded EPDM weather-strips, Polym. Eng. Sci. 53 (2013) 353–369, https://doi.org/10.1002/pen.23270.

[29] X. Sun, A.I. Isayev, Cure kinetics study of unfilled and carbon black filled synthetic isoprene rubber, Rubber Chem. Technol. 82 (2009), https://doi.org/10.5254/1.3548241.

[30] G. Milani, F. Milani, Relation between activation energy and induction in rubber sulfur vulcanization: an experimental study, J. Appl. Polym. Sci. 138 (2021) 50073, https://doi.org/10.1002/app.50073.

[31] G. Milani, F. Milani, Genetic algorithm for the optimization of rubber insulated high voltage power cables production lines, Comput. Chem. Eng. 32 (2008) 3198–3212, https://doi.org/10.1016/j.compchemeng.2008.05.010.